Dynamic-Statistic Combined Ensemble Prediction and Impact Factors on China's Summer Precipitation

Xiaojuan Wang[1], Zihan Yang[2*], Shuai Li[3], Qingquan Li[3], Guolin Feng[3, 4*]

1 College of Electronic and Information Engineering, Changshu Institute of Technology, Suzhou, 215506, China

2 Department of Atmospheric Sciences, Yunnan University, Kunming, 650500, China

3 Laboratory for Climate Research, National Climate Center, Beijing, 100081, China

4 College of Physical Science and Technology, Yangzhou University, Yangzhou, 225009, China

Abstract The dynamic-statistic prediction shown excellent performance on monthly and seasonal precipitation prediction in China and has been applied on several dynamical models. In order to further improve the prediction skill of summer precipitation in China, the Unequal-Weighted Ensemble prediction (UWE) using outputs of the dynamic-statistic prediction is presented, and its possible impact factors are also analyzed. Results indicate that the UWE has shown promise in improving the prediction skill of summer precipitation in China, on account to the UWE can overcome shortcomings of the structural inadequacy of individual dynamic-statistic prediction, reducing formulation uncertainties, resulting in more stable and accurate predictions. Impact factors analysis indicates that 1) the station-based ensemble prediction with ACC being 0.10-0.11 add PS score being 69.3-70.2, has shown better skills than the grid-based one, as the former produces probability density distribution of precipitation being closer to the observation than the latter. 2) The use of the spatial average removed anomaly correlation coefficient (SACC) may lower the prediction skill and introduce obvious errors on estimating the spatial consistency of prediction anomalies. SACC could be replaced by the revised anomaly correlation coefficient (RACC), which is calculated directly using the precipitation anomalies of each station without subtracting the average precipitation anomaly of all stations. 3) The low dispersal intensity among ensemble samples of UME implies the historical similar error selected by different approach is quite close to each other, making the correction on the model prediction is more reliable. Therefore, the UWE is expected to further improve the accuracy of summer precipitation prediction in China by considering impact factors such as the grid

Zihan Yang
2622261772@qq.com
Guolin Feng
fenggl@cma.gov.cn

or station-based ensemble approach, the method of calculating the ACC, and the dispersal intensity of ensemble samples in the application and analysis process of UWE.

Keywords: Dynamic-statistic prediction, Unequal weighted ensemble prediction, Prediction accuracy, Dispersal intensity, Revised anomaly correlation coefficient

Introduction

Accurate prediction of summer precipitation across China is paramount for dealing with critical issues such as flood and drought management, economic development, and ensuring food security. However, this task is fraught with challenges due to the intricate interplay among various atmospheric circulation components, including the East Asian summer monsoon (Ding 1994, Lu 2005), the Northwest Pacific subtropical high (Tao 2006), and the East Asia-Pacific teleconnection patterns (Huang 1987, Huang 2004). Additionally, external influences, such as the El Niño-Southern Oscillation (ENSO) (Sun, Yang et al. 2021) and the snow cover on the Tibetan Plateau (Si and Ding 2013), further complicate the prediction process. Some studies have also shown that improving the Real-time Multivariate Madden-Julian Oscillation (RMM) index or introducing better intraseasonal signal extraction methods may allow for higher predictability limits in real-time forecasting (Ding and Seo 2010). Due to these complexities, increasing the accuracy of summer rainfall prediction in China still faces challenges, the pursuit of more precise summer rainfall predictions in China is an endeavor that warrants the utmost attention from climate scientists (Wang, Schepen et al. 2012, Gong, Hutin et al. 2016).

Over the past few decades, there has been a remarkable progression in the foundation of observational data and theoretical understanding, which has significantly enhanced the capabilities of climate dynamical models in predicting seasonal rainfall (Wu, Vitart et al. 2017, Gettelman, Geer et al. 2022). High-resolution climate simulations, such as those with atmospheric resolutions of approximately 50 km and oceanic resolutions of 0.25°, have been successfully implemented by several research institutions (Satoh, Tomita et al. 2014, Roberts, Hewitt et al. 2016, Wu, Yu et al. 2021). These dynamic models have also demonstrated success in long-term prediction of atmospheric circulation patterns and sea surface temperatures in low-latitude regions (Zhu and Shukla 2013). However, the current performance of seasonal predictions for key climate elements, including rainfall and temperature, particularly in monsoon-influenced areas like East Asia (Wang, Fan et al. 2015, Gong, Dogar et al. 2017), remains somewhat constrained due to inherent limitations in parameterization schemes and the challenges associated with boundary value problems (Wang, Fan et al. 2015). This has spurred meteorologists to delve deeper into understanding how to effectively enhance the seasonal prediction skills of climate

models to better align with the needs of end-users (Gong, Hutin et al. 2016). It is well recognized that regional climate characteristics can significantly influence local rainfall patterns, atmospheric predictability varies significantly between regions, altitudes and seasons (Li and Ding 2011). Despite this, dynamic models still struggle to accurately capture these nuances, suggesting that there is potential for improvement in rainfall prediction through a statistical-dynamic approach (Specq and Batté 2020). This integrated methodology could provide a more robust framework for prediction, ultimately leading to more reliable and actionable climate predictions. The relative impact of initial condition and model uncertainties on local predictability also varies with the system state. Therefore, strategically reducing uncertainties in sensitive regions can effectively improve forecasting skills (Li, Ding et al. 2020). Apart from that, warm events are easier to predict than cold events (Li, Ding et al. 2020).

To enhance the precision of rainfall prediction, Chou (1974) initially suggested the integration of dynamical model data with statistical analogue information. This approach leverages the prediction errors from historical years with analogous initial conditions, such as similar circulation anomalies, snow cover, and sea surface temperatures (SST), to refine dynamic-analogue correction techniques. For instance, Huang, Yi et al. (1993) introduced the evolutionary analogue-based multi-time prediction method, (Ren and Chou 2006, Ren and Chou 2007) employs historical analogue data to estimate model errors in accordance with the atmospheric analogy principle, (Feng, Zhao et al. 2013, Feng, Yang et al. 2020) further develops this concept with their correction method focused on key regional impact factors. Wang and Fan (2009) proposed a scheme that integrates model forecasts with the observed spatial patterns of historical "analog years," while Gong, M. et al. (2018) advanced the leading mode-based correction method. In addition to these advancements, dynamic-statistic correction methods have been successfully applied to rainfall predictions in regions such as North China (Yang, Zhao et al. 2012) and Northeast China (Xiong, Feng et al. 2011). Furthermore, the application of these dynamic-statistic prediction has been extended to seasonal predictions, including those for autumn, winter, and spring (Lang and Wang 2010). At the Beijing Climate Center, various error selection methods have been operationalized in rainfall prediction, including the raw field-based similar error selection method, the empirical orthogonal function-based similar error selection method, the grid-based similar error selection method, the regional key impact factors-based similar error selection method,

and the abnormal factor-based similar error selection method (Feng, Yang et al. 2020). These innovative approaches underscore the ongoing efforts to harness both dynamical and statistical insights to achieve more accurate and reliable rainfall predictions.

Research has consistently demonstrated the benefits of integrating predictions from multiple climate models. For instance, the Bayesian model averaging approach (Luo, Wood et al. 2007) and the moving coefficient ensemble approach (Yang, Bai et al. 2024) are two such approaches that have shown promise. The use of a multi-model ensemble can mitigate the collective local biases that can occur in space, time, and across different variables when using individual models (Krishnamurti, Kumar et al. 2016). This approach not only assigns higher weights to the outputs of more accurate models but also enhances overall predictive skill and reduces the uncertainty associated with single-model ensembles (Yan and Tang 2013). By accounting for comprehensive uncertainties stemming from both model discrepancies and initial conditions, multi-model ensembles often outperform single models (Palmer, Alessandri et al. 2004). Furthermore, the diverse assumptions inherent in different model frameworks can potentially compensate for our incomplete understanding of atmospheric dynamics (Yan and Tang 2013). The multi-model approach has been successfully applied across a broad spectrum of forecasting needs, including medium-range weather forecasting (Candille 2009) and seasonal climate prediction (Vitart 2006). Given the aforementioned advantages of dynamic-statistic methods in seasonal predictions, it is imperative to adopt an ensemble approach that combines the predictions from these methods. This integration is crucial for further enhancing prediction accuracy and reliability. By leveraging the collective strengths of various models and techniques, we can achieve a more robust and nuanced understanding of climate patterns, ultimately leading to improved prediction capabilities.

In the process of examining the ensemble prediction, it is crucial to take into account the various factors that can influence its predictive accuracy (Krishnamurti and Kumar 2012). The ensemble's output is particularly sensitive to several key elements: the number of models incorporated, the duration of the dataset utilized for training, and the distribution of weights for both downscaling and the integration of multiple models or schemes (Krishnamurti, Kumar et al. 2016). Both grid-based reanalysis data and station-based observational data can serve as the foundation for model training or validation (Ding, Li et al. 2004, Wang, Fan et al. 2015, Gong, Hutin

et al. 2016). It is therefore essential to explore and discuss the differential impact that the use of these two distinct types of datasets may have on ensemble predictions. Furthermore, the dispersion of samples across different models or methodologies cannot be overlooked, as it also affects the ensemble's predictive skill, and deserve certain attention (Houze, Rasmussen et al. 2015).

Based on above statement, the aim of this research is to construct an Unequal-Weighted Ensemble prediction (UWE) employing a comprehensive array of dynamic-statistic methods and to explore the potential factors that may influence its predictive capabilities. Specifically, the study is designed to delve into three primary areas: (1) Elucidate the process of establishing the UWE through a suite of dynamic-statistic methods, highlighting the distinctions between grid-based ensembles and station-based ensembles. (2) Examine the most effective methodologies for evaluating the spatial congruence between observational data and the UWE's output. (3) Investigate the connection between the dispersal of samples across various dynamic-statistic methods and the predictive accuracy of the UWE. This study will provide a comprehensive analysis of the UWE's development and its performance, offering valuable insights into the factors that influence its predictive success.

1 Data and Method

1.1 Data

The monthly precipitation data of 1634 stations during 1983–2020 are from the National Meteorological Information Center of the China Meteorological Administration. The monthly grid precipitation data during 1983–2020 is derived from the Combined Rainfall Analysis (CMAP) data of the U.S. Climate Prediction Center. The model prediction data for summer precipitation in China are hindcast datasets of the BCC_CPSv3. Monthly climate indices during 1983–2020 including circulation indices (i.e. AO, AAO), SST indices (i.e. Nino 3.4, Nino 4, Pacific Decadal Oscillation), snow cover indices (i.e. Tibet snow cover area index, Northeast China snow cover area index) is available from the Beijing Climate Center website (http://cmdp.ncc-cma.net/Monitoring/ cn_index_130.php) (Gong, Hutin et al. 2016).

1.2 Climate regions division

Climate in China influence by various climate systems, such as the Monsoon, mid-high latitude circulation system and westly jet circulation system, etc. (Ding 1994,

Li, Dai et al. 2008, Wu, Vitart et al. 2017). Since summer rainfall has regional characteristics and potential impact factors, we divide the whole country into 8 regions (Feng, Yang et al. 2020) in terms of South China (110º~120ºE, 20º~25ºN), East China (110º~123ºE, 25º~35ºN), North China (110º~123ºE, 35º~42.5ºN), Northeast China (110º~135ºE, 42.5º~55ºN), Eastern Northwest China (90º~110ºE, 35º~43ºN), Western Northwest China (75º~90ºE, 35º~48ºN), Tibet Area (80º~100ºE, 27º~35ºN and Southwest China (95º~110ºE, 22º~33ºN). Each region is treated separately by the dynamic-statistic prediction process.

1.3 The dynamic-statistic predictions

Numerical model is an approximation of the behavior of the actual atmosphere. The dynamic-statistic prediction is to utilize the information of historical analogues to estimate model's prediction errors through the statistical method, thereby to compensate the model deficiencies and reduce the model errors (Huang, Yi et al. 1993). As addressed by Feng, Yang et al. (2020), the dynamic-statistic prediction can be explained by equation (1),

$$\hat{p}(\psi_0) = p(\psi_0) + \tilde{p}(\psi_j) - p(\psi_j), \quad (1)$$

Where $\hat{p}(\psi_0)$ is the corrected prediction, $p(\psi_0)$ is the original model prediction, and $p(\psi_j)$ is the model prediction of historical year having the similar initial conditions as current one, $\tilde{p}(\psi_j)$ is the corresponding historical observation. Eq. (1) is the integral form of the similarity error correction equation, in which the error term of the similar historical prediction $\tilde{p}(\psi_j) - p(\psi_j)$ is added to the prediction results of the numerical model.

$$\hat{p}(\psi_0) \xrightarrow{Estimate} \hat{E}(\psi_0), \quad (2)$$

The core idea of the dynamic-statistic prediction is developing the scheme how to select the similar year and estimate historical prediction errors(Feng, Zhao et al. 2013, Gong, Hutin et al. 2016). Eq. (2) transforms improvement in the dynamical model prediction into the estimation of model error (Ren and Chou 2006, Xiong, Feng et al. 2011, Feng, Zhao et al. 2013).

1.4 Schemes for the dynamic-statistic prediction

Fig.1 presents the flow chart of the dynamic-statistic prediction method. The key step is the scheme for selecting the historical similar years, which is the step in the red box. Different scheme of selecting similar years from the historical dataset

corresponds to different dynamic-statistic prediction scheme. In previous years, a series of the dynamic-statistic prediction schemes has been developed for selecting similar years from the historical information, and excellent results have been achieved in predicting summer precipitation anomalies in China (Wang and Fan 2009, Xiong, Feng et al. 2011, Feng, Zhao et al. 2013, Wang, Fan et al. 2015).

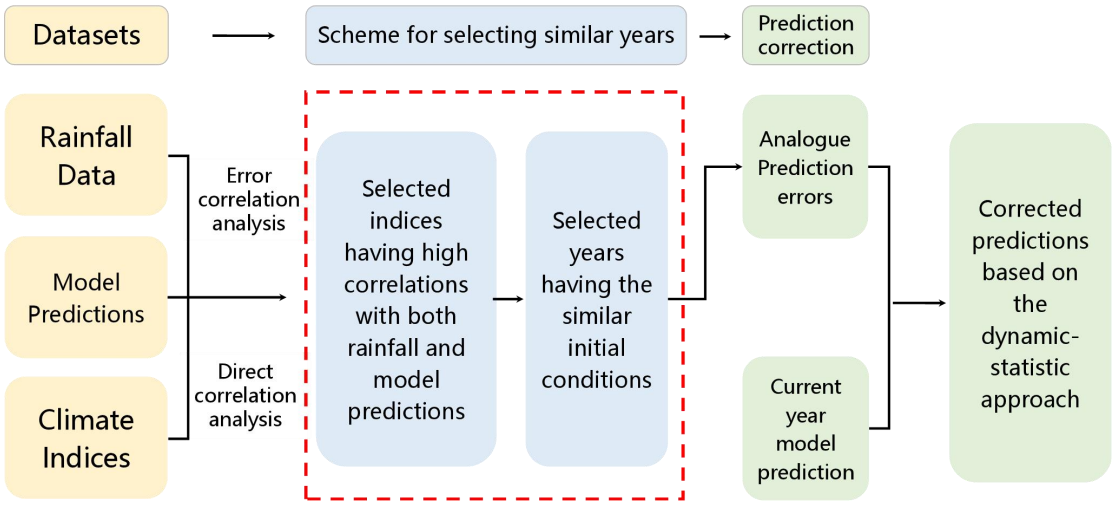

Fig. 1 The flow chart of the dynamic-statistic prediction method. The key step is the scheme for selecting the historical similar years, which is the step presented in the red dash box. The climate indices refer to the 130 monthly climate indices in terms of the SST indices, Circulation indices etc. during 1983–2020 in section 1.1

Five kinds of the dynamic-statistic prediction approach representing different scheme for analogue error selection are introduced as follows,

1) The scheme for original model prediction-based similar error selection (ORM). With the dynamical model original prediction, select four historical years has the most similar feature of anomaly distribution as the current year's prediction. Then calculate the analogue prediction error using these similar years, add to the current prediction and produce the corrected prediction.

2) The scheme for Empirical Orthogonal Function mode-based similar error selection (EOF). Calculating the model prediction error filed and produce the corresponding spatial modes and corresponding principal components using the EOF method. Similar years is selected based on the Euclidean distance of the principal components. Historical similar error is calculated using the selected similar years and added to the current model prediction, which then produce the corrected prediction

(Gong, M. et al. 2018).

3) The scheme for the regional average precipitation-based similar error selection (REG). Dividing the whole country into 8 regions using according to the introduction of section 1.2. Selecting the climate indices having high correlations with the regional average precipitation of each region. With these highly correlated indices, multi-factors are randomly configurated and used to calculate the shortest Euclidean distance to choose the historical similar years and produce the similar error. Cross-validation are carried out to correct the model prediction error and obtain the optimal multi-factor configuration. Based on this final optimal multi-predictor configuration, the dynamic-statistic prediction can be implemented (Xiong, Feng et al. 2011).

4) The scheme for the grid precipitation-based similar error selection (GRD). The similar error selection is the same as the REG approach, but the model prediction error correction is carried out on each grid point within a region.

5) The scheme for the abnormal factors based similar error selection (ABN). Establish factors having significant correlations with the regional precipitation. Determine the anomaly threshold of each factor and select the key factors reaching the threshold. Based on the selected abnormal factors, similar years are selected by the shortest Euclidean Distance of factor set between current year and historical years. Then the analogue errors can be calculated by using the method of weighted average integration and be added on the current year's model prediction, which can produce the corrected prediction (Feng, Yang et al. 2020).

6) The scheme for systematic error selection (SYS). The arithmetic mean of the model prediction errors over the years is calculated, after which it is superimposed on the model's original prediction results to obtain the systematic error revised prediction of the systematic error revised prediction of the model. This scheme is primarily used for comparison with the other five dynamic-statistic schemes.

The selected similar years are not consistent with each other among these five schemes, the analogue errors usually show similar pattern, but have difference in detail. Besides the dynamic-statistic prediction, the system error correction are also presented for comparation.

1.5 The Dynamic-Statistic Combined Ensemble Prediction

In order to further improve the effectiveness of summer precipitation prediction by various dynamic-statistic schemes, this study conducted the Dynamic-Statistic

Combined Ensemble Prediction called Unequal-Weighted Ensemble prediction (UWE).

Based on the five the dynamic-statistic prediction schemes, the unequal weighting ensemble prediction (UWE) E_m is calculated as equation (3),

$$E_m = \sum_{k=1}^{n} w_{km} F_{km} \quad (n = 5) \quad , \qquad (3)$$

Where F_{km} is the single prediction of each dynamic-statistic scheme and w_{km} is the weight coefficient of each member. n denotes the total number of dynamic-statistic scheme, m denotes the current prediction year. w_{km} can be calculated using equation (4). Using a method similar to the cross check, the TCC was calculated by removing the precipitation predictions of the screened members along with the precipitation actuals for the m th ($\mathrm{m} \in [1,10]$) year of data.

$$w_{km} = \frac{T_{km}}{\sum_{k=1}^{n} | T_{km} |} \qquad (4)$$

The weights w_{km} were calculated for each member at each grid-point in the year m, where T_{km} is the TCC value calculated for the *k*nd member at that station or grid point after excluding the precipitation data in year m, and $w_{\mathrm{km}}(k = 1,2,...,n)$ is the weight of the *k*rd member at that grid-point in year m. The anomaly correlation coefficient (ACC), PS score, and root mean standard error are used for evaluating the prediction skill for summer precipitation in China. The PS score can be calculated using equation (5).

$$PS = \frac{f_0 \times N_0 + f_1 \times N_1 + f_2 \times N_2}{N - N_0 + f_0 \times N_0 + f_1 \times N_1 + f_2 \times N_2 + M} \times 100 \, , \qquad (5)$$

Where N is the total number of stations, is the number of the correctly predicted stations with abnormal within (-20%, 20%), f_0 is weight coefficient of N_0 ; N_1 and f_1 are for the stations with abnormal within (-50%, -20%) or (20%, 50%); N_2 , f_2 are for the stations with abnormal within (-100%, -50%) or (50%, 100%); M is the total number of correctly predicted stations with abnormal below -100% or above 100%. In this study, we set $f_0 = 2$, $f_1 = 2$ and $f_2 = 4$.

Normally, the spatial average removed ACC (SACC) is calculated by formular (6)

to assess the spatial consistency of prediction for summer precipitation in China (Xiong, Feng et al. 2011, Fan, Liu et al. 2012).

$$R = \frac{\sum_{i=1}^{n}(x_i - \bar{x}_s)(y_i - \bar{y}_s)}{\sqrt{\sum_{i=1}^{n}(x_i - \bar{x}_s)^2 \sum_{i=1}^{n}(y_i - \bar{y}_s)^2}}, \quad (6)$$

Where n is the total number of stations, x_i is the summer precipitation abnormal of observation at station i, while y_i is the summer precipitation abnormal of prediction at station i. $\overline{x_s}$ and $\overline{y_s}$ are respectively the average abnormal of observation and prediction for all the stations. This so-called SACC need to subtract the average precipitation anomaly of all stations from precipitation anomaly of each station before calculating the ACC.

In order to confirm if the SACC can properly estimate the spatial consistency of prediction for summer precipitation, we also calculated the revised anomaly correlation coefficient (RACC) using formular (7),

$$R^* = \frac{\sum_{i=1}^{n}(x_i^o - \bar{x}_{i,t})(y_i^o - \bar{y}_{i,t})}{\sqrt{\sum_{i=1}^{n}(x_i^o - \bar{x}_{i,t})^2 \sum_{i=1}^{n}(y_i^o - \bar{y}_{i,t})^2}} \quad (7)$$

Where n is the total number of stations, x_i^o and y_i^o are respectively the summer precipitation of observation and prediction at station i. $\bar{x}_{i,t}$ and $\bar{y}_{i,t}$ is the average of observation and prediction of summer precipitation for all the years at each station i. The RACC is calculated directly using the precipitation anomalies of each station without removing the average precipitation anomaly of all stations.

2 The summer precipitation prediction using the dynamic-statistic scheme

The RACCs and PSs of the summer precipitation in China produced by the five dynamic-statistic methods are presented in Table 1. The 10-year average of PS score of the dynamic-statistic methods varied from 67.4-69.6, which have the better performance than that of the SYS method (65.8). In figure 2, the temporal correlation coefficients of the dynamic-statistic methods are higher than the SYS method over most China with the distribution spatial pattern is similar to each other, but the most improved areas varied among different method. It is further confirmed with previous studies that the merger of prediction error estimated via the statistical method and dynamic model-based original output represents a potential means for improving prediction skill of summer rainfall in China (Feng, Yang et al. 2020).

Table 1 10-year average of RACC and PS of the summer precipitation prediction from 2011 to 2020 for the dynamic-statistic predictions and system error correction.

Scheme	**ORM**	**EOF**	**REG**
RACC	0.10	0.03	0.01
PS	69.5	69.6	67.4
Scheme	**GRD**	**ABN**	**SYS**
RACC	0.05	0.02	-0.08
PS	68.2	69.4	65.8

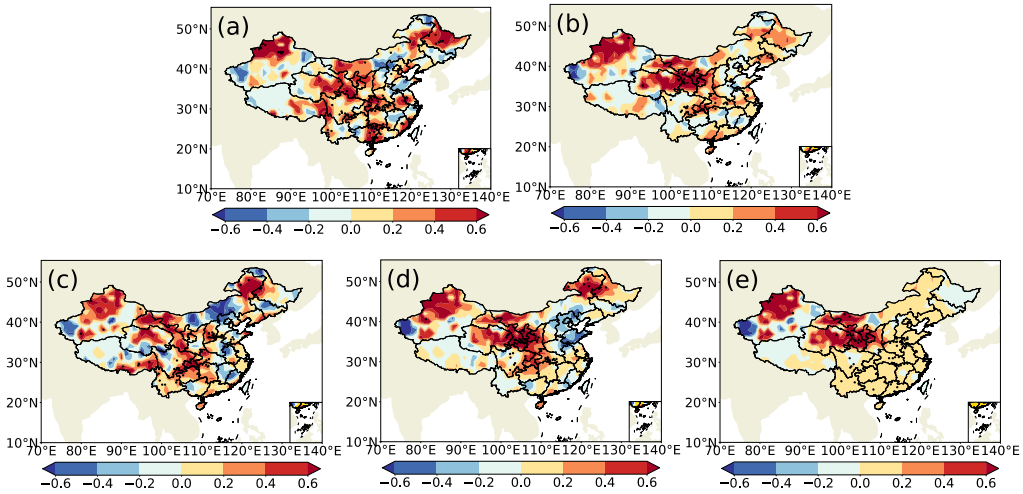

Fig. 2 The differences of the temporal correlation coefficients for summer precipitation predictions in China from 2011 to 2020. Values indicate differences of the dynamic-statistic method minus the SYS method. (a) ORM, (b) EOF, (c) REG, (d) GRD, and (e) ABN.

Based on the equation of formular (1), four schemes of UWE prediction using the single dynamic-statistic predictions as ensemble members and their corresponding one year out cross validations are presented in Table 2. In order to distinguish the performances UWE prediction against the grid-point observation and station observation, both the grid-based ensemble and station-based ensemble are calculated. Comparing with the single scheme of the dynamic-statistic prediction, the E4 scheme has the best skill among the four ensemble schemes, with RACC being 0.9 and PS score being 70. The grid-based ensemble can somewhat improve the summer precipitation prediction in China, but its effect varied among different schemes. The

skills of the station-based ensemble are obviously better than the grid-based one, with RACC being 0.10-0.11 add PS score being 69.3-70.2. As addressed by Yan and Tang (2013) the multi-model ensemble approach (MME) considers the structural inadequacy of individual models and can reduce model formulation uncertainties. The reason why the ensemble of multiple dynamic-statistic predictions can improve the summer precipitation in China is similar to that of MME, which can somewhat overcome the shortcomings of a single prediction and produce the more stable prediction.

Table 2 10-year average of RACC and PS score of summer precipitation prediction of the four UWE in China during 2011 ~ 2020.

Ensemble Scheme	Ensemble member	Grid Ensemble		Station Ensemble	
		RACC	PS	RACC	PS
E1	ORM, GRD	0.04	69.2	0.11	69.3
E2	ORM, GRD, EOF	0.07	69.3	0.11	70.2
E3	ORM, GRD, EOF, REG	0.08	69.9	0.11	70.7
E4	ORM,GRD,EOF,REG,ABN	0.09	70.0	0.10	70.1

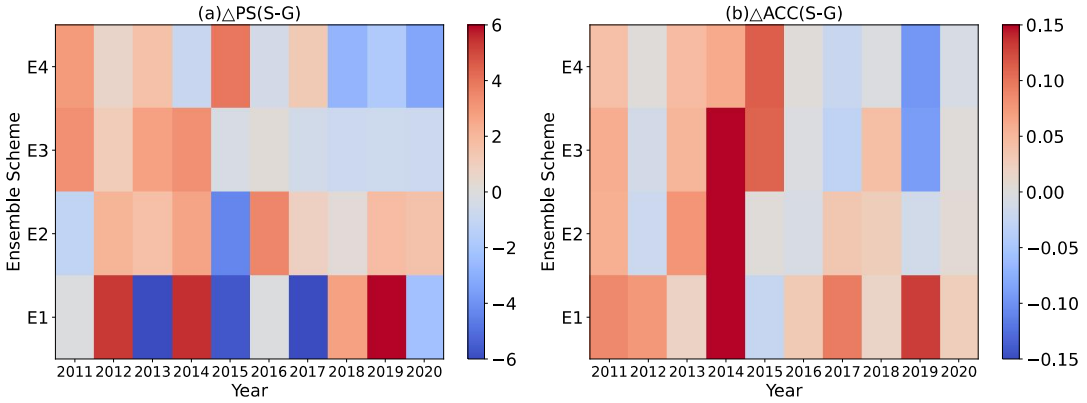

Fig. 3 Scatter distribution of differences of (a) PS and (b) RACC for summer precipitation prediction during 2011-2020 between station-based and grid-based UWE. Values indicate the differences of station-based ensemble minus the grid-based ensemble.

Figure 3 shows that there is no significant difference between the PS scores of the station-based and grid-based UWE for the E1 scheme. However, for the E2

scheme, the station-based UWE clearly outperforms the grid-based UWE. Additionally, the station-based UWE of E3 and E4 schemes also has relatively higher PS scores. RACC values, of the station-based prediction for all four schemes are generally higher than those for the grid-based UWE. In summary, compared to the grid-based UWE, the station-based one have obvious higher PS scores and RACC values, indicating better prediction performance.

In Fig. 4, the TCC of the station-based ensemble for summer precipitation prediction show positive values in most China, with the high value centers distributed in western South China, central China, southern North China and western Northeast China, etc. The similar spatial distributions are observed in predictions of the four station-based ensemble schemes (Fig. 4 a, c, e, g). The TCC differences between the station-based ensemble and the grid-based ensemble indicate that the former has higher than values than the later in most areas of China, except for part of Central China and East China (Fig. 4 b, d, f, h). The spatial distribution of TCC indicates the improvement of the station-based ensemble is suitable for most stations in China and implies this approach can make the summer precipitation prediction being closer to the observation. Bueh, Shi et al. (2008) also addressed that the training phase of multi-model ensemble learns from the recent past performances of models and is used to determine statistical weights from a least square minimization via a simple multiple regression. During the training process, more precise objective data can produce better weight coefficients and lead to more accurate ensemble result, which might be the reason for the station-based ensemble produce better predictions of summer precipitation in China than the grid-based one.

Fig.5 indicates that the probability density distribution of station-based ensemble predictions is closer to the observation especially at the peak part than the gird-based ensemble and this feature is observed in four ensemble predictions. If the onsite observation dataset can be used for training, we may have a parameterization scheme containing precise information for each single station, which may be of help to produce the prediction being close to the real situation of summer precipitation in China. Since the gird-based dataset normally is the reproduced observation data, which may lose certain precise information especially for those extreme values. This flaw of the grid data may cause it to have poor performance on improving the prediction accuracy than the station data(Xiong, Feng et al. 2011, Kim, Webster et al. 2012, Yang, Bai et al. 2024).

The station-based and grid-based UWE, as well as the actual precipitation data, all exhibit characteristics of a normal distribution in Fig.5, instead of the typical skewed distribution. This is primarily because this study focuses on summer precipitation over the entire China region, which covers a large area and spans a long period rather than the precipitation in a single grid or station in a short period. Within this range, various types of precipitation events, including light, moderate, and heavy rain, make the probability distribution closer to the normal distribution. Besides, In Fig. 5, probability distribution is calculated based on the monthly anomaly precipitation, and after a treatment of probability function of python program, which smooth the distribution curve. Therefore, the final probability distribution appears as a normal distribution.

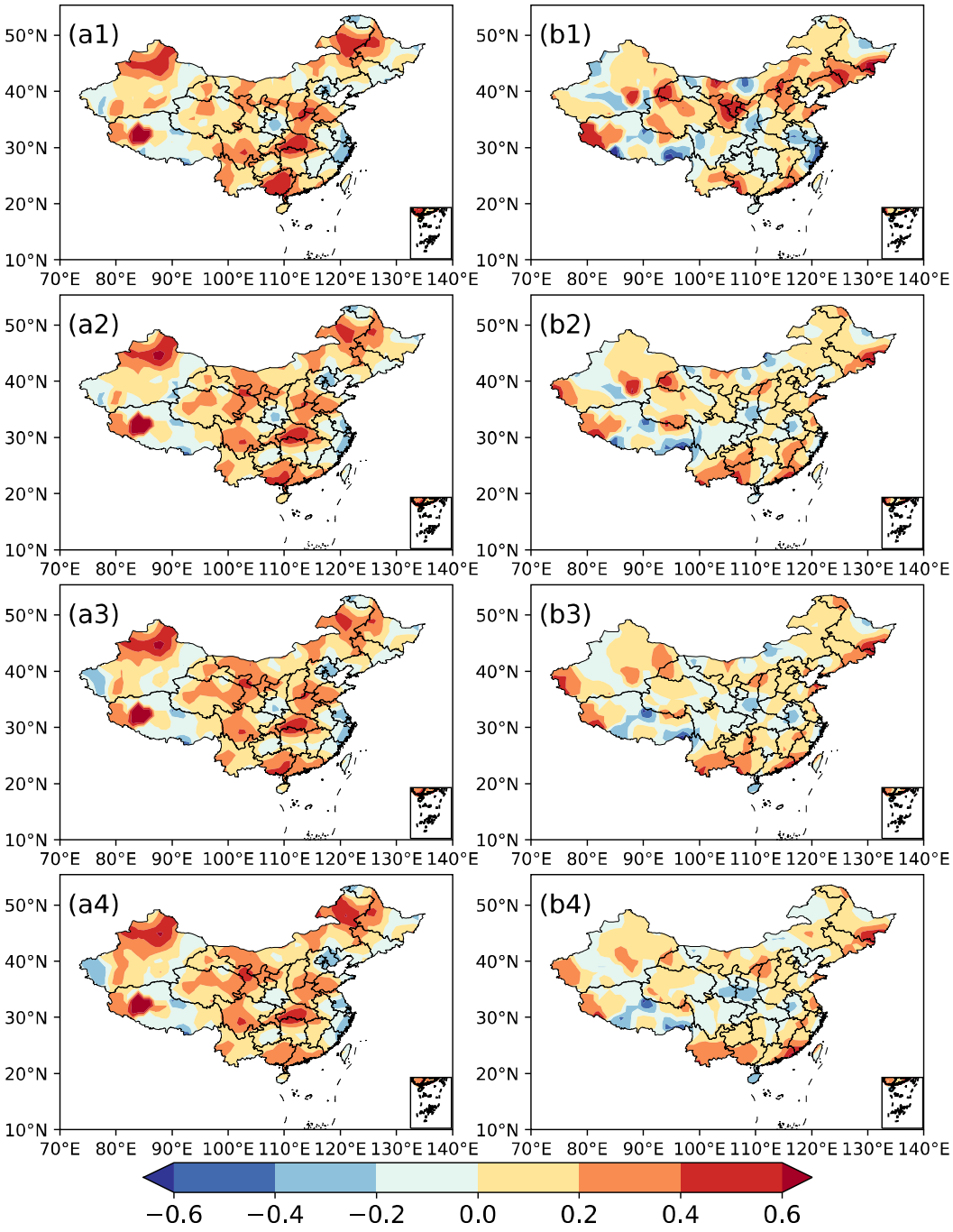

409

410 **Fig. 4** Spatial distribution of TCC of station-based UWE for summer precipitation in
411 China during 2011-2020 (a1-a4), TCC differences of station-based ensemble minus
412 the grid-based ensemble (b1-b4). (a1, b1) Ensemble scheme E1; (a2, b3) Ensemble
413 scheme E2; (a3, b3) Ensemble scheme E3; (a4, b4) Ensemble scheme E4.

414

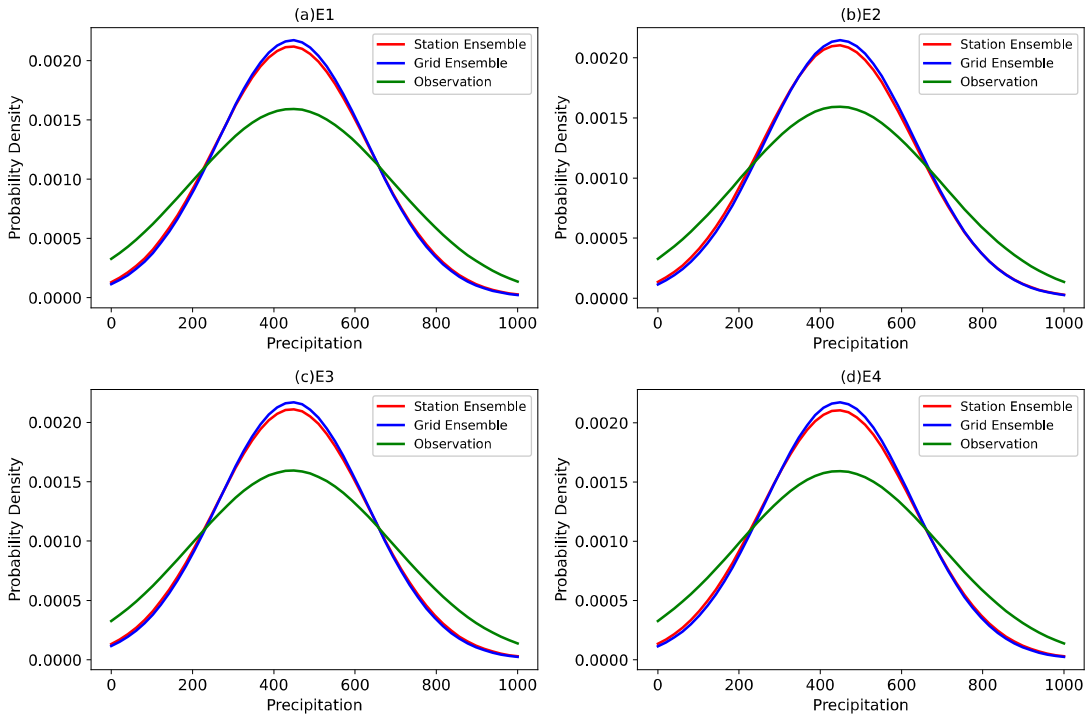

Fig. 5 Probability density distribution of the total precipitation for observation and UWE. (a) Ensemble Scheme E1, (b) Ensemble Scheme E2, (a) Ensemble Scheme E3, (a) Ensemble Scheme E4.

3 Calculating the spatial similarity of ensemble prediction.

In Fig. 6, the SACCs and RACCs are not consistent with each other, and the former are more frequently lower than the latter. The 10-year average values of SACC for each ensemble prediction for summer precipitation in China are also lower than the RACC (table 1). The SACC is calculated after subtracting the spatial average of anomaly for all the stations from the original precipitation anomaly. This approach may cause the new value for each station can't reflect the real situation and lead to a decrease of RACC between the prediction and observation. In fig.7 the correlation between the RACC and PS are all higher than those between the SAAC and PS, which further indicated RACC can better assess the prediction skill of summer precipitation. It is also noted that the differences between the SACC and RACC are quite obvious in 2011 and 2015 for ensemble schemes E2, E3, and E4 (Fig. 6 b, c, d). Comparing with the PS scores, it seems that the RACC for each prediction have more consistent feature than the SACC. In order to figure out if the RACC has the better performance than the SACC on indicating the spatial consistency of precipitation prediction, the observation and prediction of summer precipitation in 2011 and 2015

436 are respectively presented in Fig. 7. Comparing with the observation (Fig. 7 a5),
437 predicted precipitation anomalies in summer 2011 show consistent feature in most
438 China (Fig. 7 a1-a4). The PS scores of four ensemble schemes are respectively 69.5,
439 68.7, 73.5, 74.3, and RACCs are 0.08, 0.07, 0.10, 0.11, which properly indicate the
440 prediction skill of these four predictions on the summer precipitation in 2011. It is
441 also noted that the SACCs of 2011 prediction are respectively 0.01, -0.08, -0.11 and
442 -0.14, which obviously have flaws in assessing the performance of these four schemes
443 on predicting the precipitation. This shortcoming of the SACC is also exhibited in the
444 prediction of summer precipitation anomalies in 2015 (Fig. 7 b1-b5), owing to its
445 improperly low SACC values being 0.01, -0.07, -0.13, -0.17, respectively.
446
447 **Table 3** 10-year average of RACC, SACC of station-based ensemble predictions for
448 summer precipitation in China during 2011-2020.

	E1	E2	E3	E4
RACC	0.11	0.11	0.11	0.10
SACC	0.10	0.08	0.07	0.05

449

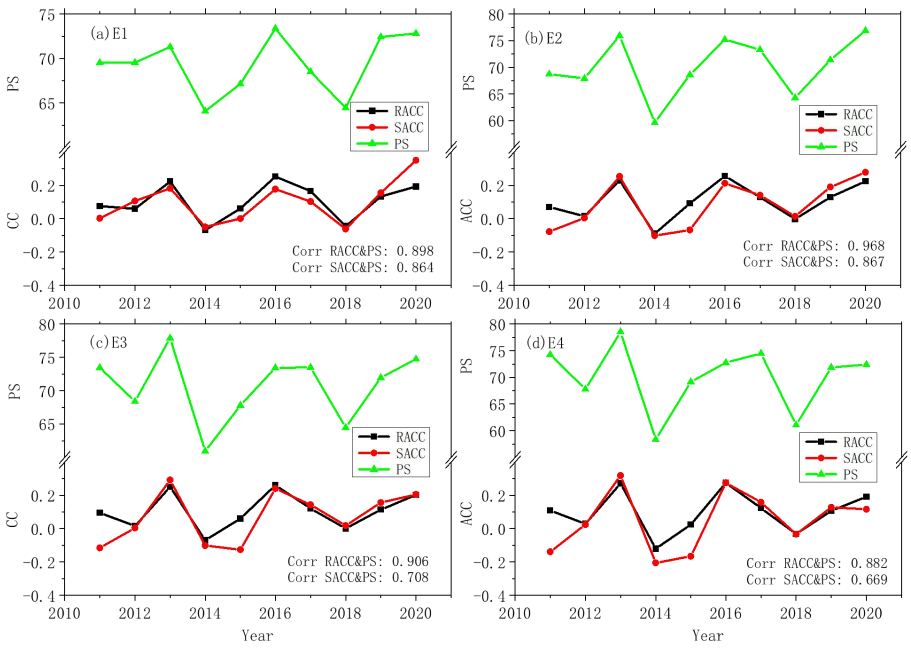

450
451 **Fig. 6** Annual **R**ACC, SACC and PS of station-based ensemble predictions for
452 summer precipitation in China. Prediction of (a) E1, (b) E2, (c) E3 and (d) E4
453 approach, respectively.

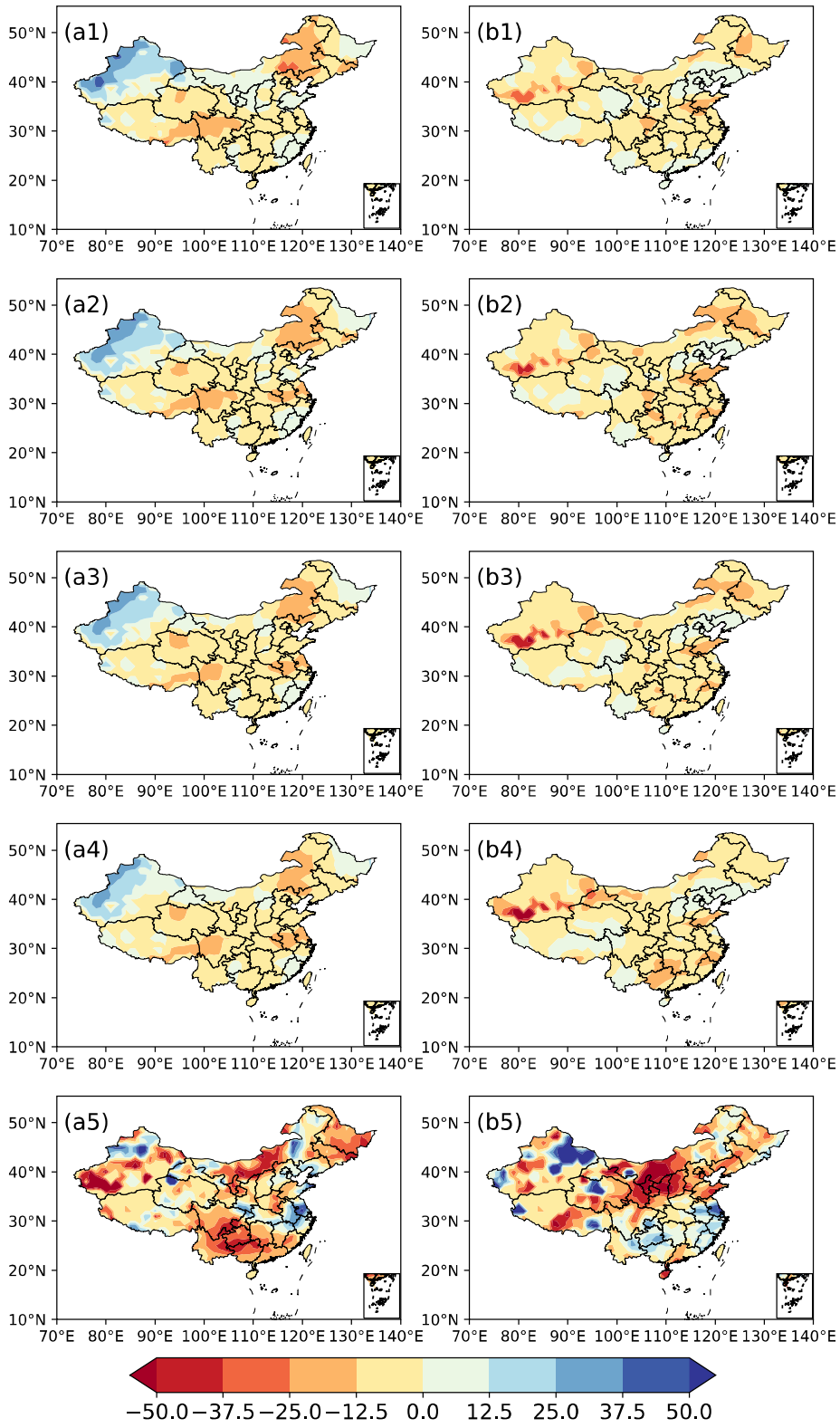

Fig. 7 The spatial distribution of anomalies (unit: %) of observation and prediction of summer precipitation in 2011 and 2015. (a1-a4) prediction of scheme E1-E4, and (a5) observation for 2011; (b1-b4) prediction of scheme E1-E4, and (b5) observation for 2015.

4. Impact of dispersal intensity on the ensemble prediction.

The dispersal intensity (Di) also called as the coefficient of variation, which is a variable measure the differences among single samples and can be calculated by formal (8). The dispersal intensity is also a relative measure of variability that indicates the size of a standard deviation in relation to its mean. It is a standardized, unitless measure that allows you to compare variability between disparate groups and characteristics (Tyralis and Papacharalampous 2024).

$$Di = \frac{\sqrt{\sum_{k=1}^{n}(F_{km} - \overline{F}_m)^2 / n}}{\overline{F}_m} \tag{8}$$

Since the dispersal intensity of each statistic-dynamic prediction has obvious interannual variation, it is necessary to analyze its probable impact on the ensemble prediction of summer prediction in China. Fig. 8 presents the relationship of ACC - dispersal intensity of summer precipitation prediction, in which high ACCs of summer precipitation prediction mostly corresponds to the low dispersal intensity among statistic-dynamic predictions. The variabilities of the signal and noise for the ensemble prediction can be measured as the variance of the ensemble mean and ensemble spread of all the initial conditions (Zheng, Wang et al. 2009, Liu, Tang et al. 2019), the sampling error on measuring the signal variance, the more reasonable estimation of the signal variance can be given and used to measure the overall potential predictability of the prediction system (DelSole 2004, DelSole and Tippett 2007). The UWE has the similar theory as the ensemble prediction, the low dispersal intensity among ensemble samples implies the historical similar error selected by different approach is quite close to each other, which makes the correction on the model prediction is more trustable and then produce a more accurate prediction than those cases with high dispersal intensity.

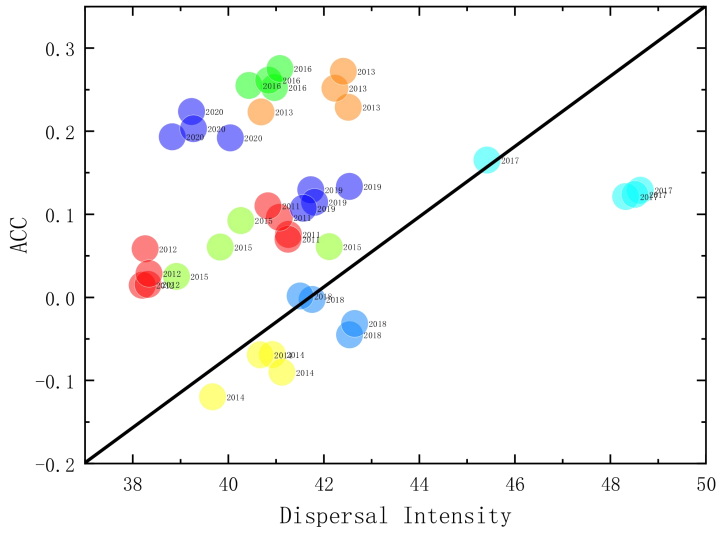

Fig. 8 The relationship between each UME's ACC and the dispersal intensity of each summer precipitation prediction during 2011-2020. The four dots of each color indicate the four schemes (E1-E4) applied in ear year's dynamic-statistic prediction.

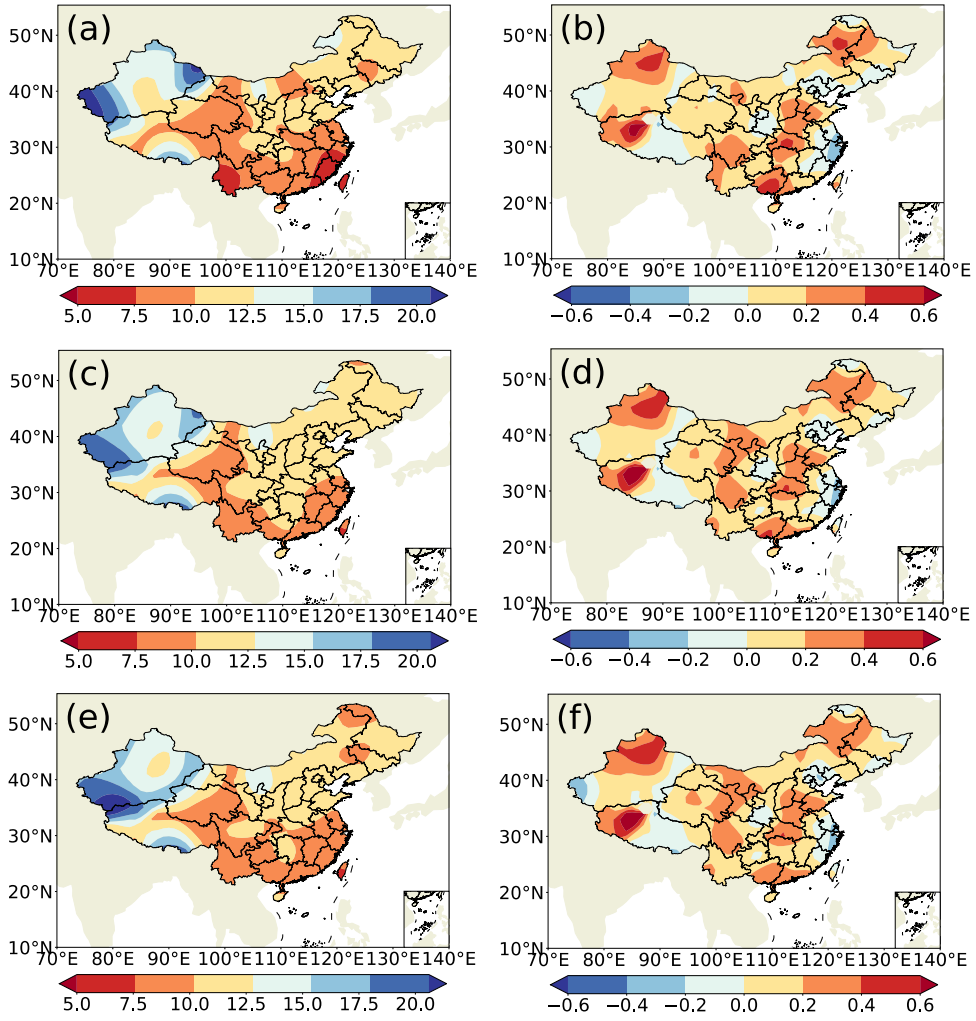

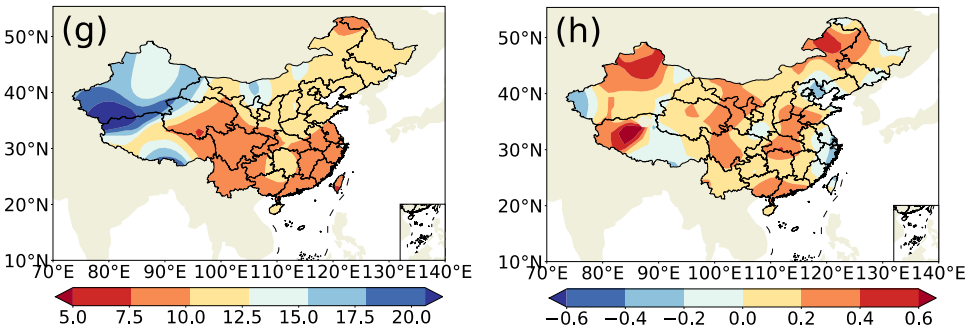

Fig. 9 The spatial distinction of the 10-year average of dispersal intensity (a, c, e, g) and TCC (b, d, f, h) of UME scheme of E1-E4 during 2011-2020.

In Fig. 9, the 10-year average of dispersal intensity of each UME scheme show the similar pattern as the spatial distribution of TCC of summer prediction produced by UME. Except for part of Northwest China and middle East China, the low dispersal intensity also tends to produce high TCC of statistic-dynamic combined ensemble prediction in most China. In the middle region of China, the negative correlation between the dispersal intensity and TCC is not so evident. This could be due to the limitations of the parameterization schemes in the forecast models for this region, which may result in inaccurate simulations of the diffusion process. Additionally, the diversity of meteorological conditions in the middle region could lead to inconsistencies in the relationship between dispersal intensity and TCC across different areas. For instance, the middle region may be influenced by specific meteorological systems, such as frontal systems and cyclones, which can affect the relationship between dispersal intensity and TCC. Therefore, the positive relationship between the dispersal intensity and the ACC can be found in this study, however this kind of relationship has uncertainty in different areas, which still need to be considered in the operational predictions. These aspects require further detailed investigation. In conclusion, The low dispersal intensity among the single prediction corresponds to the major physical process captured by each prediction scheme is similar with each other, which is help of the more reasonable estimation of the signal variance and produce the better precipitation predictions.

5. Conclusions and discussion

This study presents the UWE of the dynamic-statistic schemes in order to enhance summer precipitation prediction in China. The analysis also includes an

examination of factors that may impact the prediction skill of UWE, such as grid-based and station-based prediction, the calculation of prediction skill, and the influence of sample dispersion on prediction accuracy.

UWE's performance surpasses the model and the dynamic-statistic scheme predictions, potentially due to its ability to overcome individual model or scheme inadequacies, reduce formulation uncertainties, and yield a more stable and accurate predictions. The average RACC and PS values for the five dynamic-statistic schemes that were ensemble members are 0.02-0.10 and 67.4-69.6. In contrast, the grid-based ensemble prediction of UWE becomes 0.04-0.09 and 69.2-70.9, which is an improvement compared to the dynamic-statistic schemes. Station-based ensemble prediction shows superior performance for this well compared to grid-based ensemble prediction and dynamic-statistic methods, achieving average RACC values of 0.10-0.11 and PS values of 69.3-70.7.

The average RACC and PS values for the station-based ensemble prediction fluctuated between 0.10-0.11 and 69.3-70.2 from 2011 to 2020, indicating significantly higher proficiency compared to the grid-based ensemble prediction. The ensemble prediction based on station data can produce precipitation with a probability density distribution function that is closer to the observed data compared to the grid-based prediction, making the former more accurate. The use of the SACC needs to remove the spatial average of the whole stations from the original value, which may produce inaccurate station values and lead to a lower correlation between predictions and observations. This makes SACC unsuitable for estimating the spatial consistency of summer precipitation predictions. The commonly used SACC should be supplanted by the updated RACC, which is computed by directly utilizing the precipitation anomalies at each station, without the need to deduct the overall average precipitation anomaly from all stations.

Moreover, the higher RACCs in summer precipitation prediction are predominantly associated with lower dispersal intensity among the dynamic-statistic predictions. This indicates that a more concentrated ensemble, where predictions are closely aligned, tends to result in more accurate forecasts. Accordingly, the dispersal intensity of ensemble samples is a crucial factor affecting the prediction accuracy of dynamic-statistic combined UWE. UWE shares a similar theoretical foundation with ensemble prediction. Low dispersal intensity among ensemble samples suggests that the historical similar errors identified by various methods are closely aligned. This

alignment enhances the reliability of corrections applied to model predictions, thereby yielding more accurate forecasts compared to cases with high dispersal intensities.

Acknowledgement，This work is supported by the National Natural Science Foundation of China Project (Nos.42130610, 42075057, and 42275050) and the National Key Research and Development Program of China (2022YFE0136000).

Author contributions. The conception of this paper is supposed by Xiaojuan Wang and Guolin. Material preparation, data collection, and analysis were performed by Xiaojuan Wang and Zihan Yang. The manuscript is written by Xiaojuan Wang and revised by Qingquan Li. All authors commented on previous versions of the manuscript. All the authors have read and approved the final manuscript.

Funding. The National Natural Science Foundation of China Project (Nos. 42130610, 42075057, and 42275050), The National Key Research and Development Program of China (2022YFE0136000).

Data Availability Statement. The datasets generated during and/or analyzed during the current study are available from the corresponding author on reasonable request.

Ethics declarations. The authors declare no conflict of interest. Authors have no additional information that might be relevant for the editors, reviewers and readers. The funding sponsors have no participation in the execution of the experiment, the decision to publish the results, nor the writing of the manuscript.

Conflict of interest: The authors have no relevant financial or non-financial interests to disclose.

Reference

Bueh, C., et al. (2008). "Features of the EAP events on the medium-range evolution process and the mid- and high-latitude Rossby wave activities during the Meiyu period." Chinese Science Bulletin **53**(4): 610-623.

Candille, G. (2009). "The multiensemble approach: The NAEFS example." Mon. Weather Rev. **137**: 1655–1665.

584 Chou, J. (1974). "A problem of using past data in numerical weather forecasting
585 (in Chinese)." **6**: 635-644
586
587 DelSole, T. (2004). "Predictability and information theory. Part I: measures of
588 predictability." J Atmos Sci **61**: 2425–2440.
589
590 DelSole, T. and M. K. Tippett (2007). "Predictability: recent insights from
591 information theory." Rev. Geophys. **45**: 4002.
592
593 Ding, R. and K. H. Seo (2010). "Predictability of the Madden-Julian Oscillation
594 Estimated Using Observational Data." Monthly Weather Review **138**(3):
595 1004-1013.
596
597 Ding, Y. (1994). "Monsoons over China. Advances in Atmospheric Sciences."
598 Advances in Atmospheric Sciences **11**: 252.
599
600 Ding, Y., et al. (2004). "Advance in Seasonal Dynamical Prediction Operation in
601 China." Acta Meteorologica Sinica **30**(5): 598-612.
602
603 Fan, K., et al. (2012). "Improving the Prediction of the East Asian Summer
604 Monsoon: New Approaches." Weather and Forecasting **27**(4): 1017-1030.
605

606 Feng, G., et al. (2020). "Improved prediction model for flood-season rainfall
607 based on a nonlinear dynamics-statistic combined method." Chaos, Solitons &
608 Fractals **140**: 110160.
609
610 Feng, G., et al. (2013). "Recent progress on the objective and quantifiable forecast
611 of summer precipitation based on dynamical statistical method." J. Appl. Meteor.
612 Sci **24**: 656-665.
613
614 Gettelman, A., et al. (2022). "The future of Earth system prediction: Advances in
615 model-data fusion." SCIENCE ADVANCES **8**: eabn3488.
616
617 Gong, Z., et al. (2017). "Limitations of BCC_CSM's ability to predict summer
618 precipitation over East Asia and the Northwestern Pacific." Atmospheric Research
619 **193**: 184-191.
620
621 Gong, Z., et al. (2016). "Methods for Improving the Prediction Skill of Summer
622 Precipitation over East Asia–West Pacific." Weather and Forecasting **31**(4):
623 1381-1392.
624
625 Gong, Z., et al. (2018). "Assessment and Correction of BCC_CSM's Performance in
626 Capturing Leading Modes of Summer Precipitation over North Asia."
627 International Journal of Climatology **38**(5): 2201-2214.

628

629 Houze, R. A., et al. (2015). "The variable nature of convection in the tropics and
630 subtropics: A legacy of 16 years of the Tropical Rainfall Measuring Mission
631 satellite." Rev. Geophys. **53**: 994–1021.

632

633 Huang, G. (2004). "An Index Measuring the Interannual Variation of the East
634 Asian Summer Monsoon—The EAP Index." Adv. Atmos. Sci. **21**(1): 41-52.

635

636 Huang, J., et al. (1993). "An analogue-dynamical long-range numerical weather
637 prediction system incorporating historical evolution." Quarterly Journal of the
638 Royal Meteorological Society **119**(511): 547-565.

639

640 Huang, R. (1987). Influence of the heat source anomaly over the tropical western
641 Pacific on the subtropical high over East Asia. International Conference on the
642 General Circulation of East Asia, Chengdu.

643

644 Kim, H.-M., et al. (2012). "Seasonal prediction skill of ECMWF System 4 and NCEP
645 CFSv2 retrospective forecast for the Northern Hemisphere Winter." Climate
646 Dynamics **39**(12): 2957-2973.

647

Krishnamurti, T. N. and V. Kumar (2012). "Improved seasonal precipitation forecasts for the Asian Monsoon using a large suite of atmosphere ocean coupled models: Anomaly." J. Clim. **25**: 65–88.

Krishnamurti, T. N., et al. (2016). "A review of multimodel superensemble forecasting for weather, seasonal climate, and hurricanes." Reviews of Geophysics **54**(2): 336-377.

Lang, X. and H. Wang (2010). "Improving Extraseasonal Summer Rainfall Prediction by Merging Information from GCMs and Observations." Weather and Forecasting **25**(4): 1263-1274.

Li, H., et al. (2008). "Responses of East Asian summer monsoon to historical SST and atmospheric forcing during 1950–2000." Climate Dynamics **34**(4): 501-514.

Li, J. and R. Ding (2011). "Temporal-Spatial Distribution of Atmospheric Predictability Limit by Local Dynamical Analogs." Monthly Weather Review **139**(10): 3265-3283.

Li, X., et al. (2020). "Quantitative Comparison of Predictabilities of Warm and Cold Events Using the Backward Nonlinear Local Lyapunov Exponent Method." Advances in Atmospheric Sciences **37**(9): 951-958.

Li, X., et al. (2020). "Quantitative study of the relative effects of initial condition and model uncertainties on local predictability in a nonlinear dynamical system." Chaos, Solitons & Fractals **139**(1).

Liu, T., et al. (2019). "The relationship among probabilistic, deterministic and potential skills in predicting the ENSO for the past 161 years." Climate Dynamics **53**(11): 6947-6960.

Lu, R. Y. (2005). "Interannual variation of North China rainfall in rainy season and SSTs in the equatorial eastern Pacific." Chinese Science Bulletin **50**(18): 2069-2073.

Luo, L., et al. (2007). "Bayesian merging of multiple climate model forecasts for seasonal hydrological predictions." J. Geophys. Res. Atmos. **112**: D10102.

Palmer, T. N., et al. (2004). "Development of a European multimodel ensemble system for seasonal-to-interannual prediction (DEMETER)." Bull. Am. Meteorol. Soc. **85**: 853–872.

Ren, H. L. and J. F. Chou (2006). "Introducing the updating ofmulti reference states into dynamical analogue prediction." ActaMeteor. Sinica **64**: 315–324.

692

693 Ren, H. L. and J. F. Chou (2007). "Strategy and methodology ofdynamical
694 analogue prediction." Sci. China (D) **50**: 1589–1599.

695

696 Roberts, M. J., et al. (2016). "Impact of ocean resolution on coupled air-sea fluxes
697 and large - scale climate." GEOPHYSICAL RESEARCH LETTERS **43**(19):
698 10,430-410,438.

699

700 Satoh, M., et al. (2014). "The non-hydrostatic icosahedral atmospheric model:
701 Description and development." Progress in Earth and Planetary Science **1**(1):
702 1-32.

703

704 Si, D. and Y. Ding (2013). "Decadal change in the correlation pattern between the
705 Tibetan Plateau winter snow and the East Asian summer precipitation during
706 1979–2011." Journal of Climate **26**(19): 7622-7634.

707

708 Specq, D. and L. Batté (2020). "Improving subseasonal precipitation forecasts
709 through a statistical–dynamical approach: application to the southwest tropical
710 Pacific." Clim. Dyn. **55**: 1913–1927.

711

712 Sun, L., et al. (2021). "Changing Impact of ENSO Events on the Following Summer
713 Rainfall in Eastern China since the 1950s." Journal Of Climate **34**(20): 8105-8123.

714

715 Tao, S. (2006). "The Westward,Northward Advance of the Subtropical High over
716 the West Pacific in Summer." Journal of Applied Meteorological Science.

717

718 Tyralis, H. and G. Papacharalampous (2024). "A review of predictive uncertainty
719 estimation with machine learning." Artificial Intelligence Review **57**(4): 94.

720

721 Vitart, F. (2006). "Seasonal forecasting of tropical storm frequency using a
722 multi-model ensemble." Q. J. R. Meteorol. Soc. **132**: 647–666.

723

724 Wang, H. and K. Fan (2009). "A New Scheme for Improving the Seasonal
725 Prediction of Summer Precipitation Anomalies." Weather and Forecasting **24**(2):
726 548-554.

727

728 Wang, H., et al. (2015). "A review of seasonal climate prediction research in
729 China." Advances in Atmospheric Sciences **32**(2): 149-168.

730

731 Wang, Q. J., et al. (2012). "Merging Seasonal Rainfall Forecasts from Multiple
732 Statistical Models through Bayesian Model Averaging." Journal Of Climate **25**(16):
733 5524-5537.

734

735 Wu, J., et al. (2017). "Simulations of the Asian summer monsoon in the
736 sub-seasonal to seasonal prediction project (S2S) database." Quarterly Journal of
737 the Royal Meteorological Society **143**: 706-727.
738
739 Wu, T., et al. (2021). "BCC-CSM2-HR: A High-Resolution Version 1 of the Beijing
740 Climate Center Climate System Model." Geosintific Model Development **14**:
741 2977–3006.
742
743 Xiong, K., et al. (2011). "Analogue-dynamical prediction of monsoon
744 precipitation in Northeast China based on dynamic and optimal configuration of
745 multiple predictors." Acta. Meteor. Sin. **25**: 316–326. .
746
747 Xiong, K. G., et al. (2011). "Analogue-dynamical prediction of monsoon
748 precipitation in Northeast China based on dynamic and optimal configuration of
749 multiple predictors." J. Meteor. Sci **25**(3): 316-326.
750
751 Yan, X. and Y. Tang (2013). "An analysis of multi-model ensembles for seasonal
752 climate predictions." Quarterly Journal of the Royal Meteorological Society
753 **139**(674): 1179-1198.
754

Yang, J., et al. (2012). "Estimating the Prediction Errors of Dynamical Climate Model on the Basis of Prophase Key Factors in North China." Chin. J. Atmos. Sci. **36**: 11-22.

Yang, Z., et al. (2024). "Analysis on the station-based and grid- based integration for dynamic-statistic combined predictions." **155**(6): 5184.

Zheng, F., et al. (2009). "ENSO ensemble prediction: Initial error perturbations vs. model error perturbations." Chinese Science Bulletin **54**(14): 2516-2523.

Zhu, J. and J. Shukla (2013). "The role of air–sea coupling in seasonal prediction of Asia–Pacific summer monsoon rainfall." Journal of Climate **26**(15): 5689-5697.